Experimental Measurements of Impinging Jet Atomization at the Vicinity of Liquid Fan

Ryota Sakisaka[1], Jun Hayashi[*1], Yu Daimon[2], Nobuhiro Yamanishi[2],
Fumiteru Akamatsu[1]
Osaka University, Japan[1], Japan Aerospace Exploration Agency, Japan[2]
sakisaka@combu.mech.eng.osaka-u.ac.jp, j.hayashi@mech.eng.osaka-u.ac.jp,
daimon.yu@jaxa.jp, yamanishi.nobuhiro@jaxa.jp, akamatsu@mech.eng.osaka-u.ac.jp

Abstract

Atomization by the impingement of two liquid jets of liquid fuel and oxidant is utilized as the primary process of combustion in the thrust chamber of satellite thruster. This atomization procedure is modeled in the computational fluid dynamics (CFD) for a development of the thruster configurations. However, it needs some adjustments for appropriate solution. It needs to adapt impinging jet atomization model to actual phenomena. In this study, experimental measurements of impingement jet atomization process, which intended to verify the reported numerical model [1], were conducted by using high-speed imaging and phase Doppler anemometry (PDA). Results clearly showed that the area of liquid fan and ligament is much smaller than that obtained from the reported numerical model. In addition, the experimental results showed that it needs to take the spatial distribution of mean droplet size of spray into consideration for developing the model of impinging jet atomization not only in the plane of liquid fan but also in the perpendicular plane of liquid fan.

Introduction

Combustion phenomena in thrust chamber of rocket engine are spray combustion of liquid oxydant and liquid fuel. Basically, spray combustion is a highly complex reactive two-phase phenomenon in which many simultaneous processes affect one another, including dispersion of fuel droplets, their evaporation, chemical reactions of the fuel vapor with the oxidizer, and combustion. Temporal and spatial spray characteristics such as droplet size distribution, mean droplet size and width of the droplet size distribution are important for characterizing spray combustion phenomena [2-18]. Greenberg and coworkers [2, 9, 12 and 13] conducted theoretical researches of spray combustion in counterflow systems and indicated that the initial spray characteristics such as mean droplet size, droplet size distribution, and droplet evaporation rate considerably influence the distributions of flame temperature and species concentrations. Bossard and Peck [18] indicated that the droplet size distribution has a direct influence on the flame structure, burning rates, and emissions of poly-disperse fuel spray flames. They also inferred that these effects stem from the different rate of evaporation and dispersion of various droplet sizes.

Since thrust force of liquid propellant thruster is produced by spray combustion of liquid oxidant and liquid fuel, it is important to understand atomization characteristics of liquid propellant thruster. Impinging jet atomizer is used in atomization of liquid propellant thruster of planetary exploration spacecraft and satellite because of a lot of advantages such as fine atomization and good spatial distribution. Breakup mechanisms of impinging jet atomizers consist of three main steps, namely formation of liquid fan, disintegrate to the liquid fragment and breakup into droplets. These processes of impinging jet atomization are affected by aerodynamic, viscous, inertial force and instability wave appeared on the liquid surface.

Basic mechanisms of impinging jet flow and impinging atomization characteristics were investigated theoretically by Dombrowski and Johns [19]. Inamura et al. conducted theoretical modeling by using the results of Dombrowski and Johns [1]. Those results are used for the development of liquid propellant thruster as the modeling with computational fluid dynamics (CFD).

A propellant thruster is used to be desinged by heuristic approaches with spending a lot of cost and time. Since the remarkable development of the CFD techniques and its equipment, heuristic approaches are going to be replaced by the combustor design using CFD [19-24]. Those reseaches, however, did not deal with the atomization process including a gas-liquid free surface in CFD because of the limitation of calculation cost. Therefore, the empirical models based on experimental results are proposed for estimating mean droplet size and droplet size distribution in CFD [25, 26]. Anderson et al. measured water spray characteristics by using phase Doppler anemometry (PDA), and proposed empirical formula for calculating mean diameter [24]. Whereas there is an inhomogeneity of mean droplet size and droplet size distribution in the azimuthal direction, most of proposed-formula give one mean diameter in initial positions. Since it is known that the differences between the actual spray characteristics and the empirical models for designing the thulust chamber, it needs to understand spray characteristics at the vicinity of liquid fan and to analyze its inhomogeneity of spray for improving the impinging jet atomization model. Therefore, the final goal of this study is to make impinging jet atomization model with using atomization processes and spray characteristics at the vicinity of liquid fan. This paper, for the first step, experimental measurements of impinging atomization processes are conducted by using high-speed imaging and PDA measurements at the vicinity of liquid fan.

Experimental Methods

Schematic diagrams of the experimental apparatus are shown in Figs. 1 (a), (b). As shown in Figs. 1 (a), (b), the experimental apparatus consists of liquid supply system, injector and optical measuring system. The supply system is composed of N_2 gas cylinder, two independent liquid tanks and mass flow controllers (HORIBA STEC, LV-F60PO/MO). Test liquids are transported from liquid tanks pressured by N_2. Flow rates of each impinging jets are carefully controlled by using mass flow controller. To keep the flow rates of liquid jets precisely, flow channels of two liquid jets are separated independently. Impinging jet atomizer has almost same size as an actual injector used in liquid propellant thruster. Injector has two holes and liquid jets are injected from each hole. Experiments are conducted under atmospheric pressure and normal temperature. Since the mixed liquid of hydrazine and nitrogen tetroxide has the hypergolicity, it needs to use the alternative liquid for elucidating the breakup processes of impinging jet atomization without effects of extra dynamics, which came from combustion phenomena, on atomization processes. In this study, water is used as the alternative liquid of both liquid jets because of it has similar physical properties with hydrazine and nitrogen tetroxide. Optical measurement system, shown in Fig. 1 (a), is composed of Ar^+ laser (Spectra Physics, Stable2017, 514.5 nm) as the light source, PDA (Dantec Dynamics, 57X10 and 58N10) with three dimensional traverse system. Spray characteristics, such as droplet size and droplet vertical velocity, are measured by PDA. For the high-speed imaging, PDA is replaced by the high-speed CMOS camera (Phantom V5.0 and Phantom V12.0, Vision Research Inc.) as shown in Fig. 1 (b). High speed imaging of atomization processes of liquid fan to spray is measured by using high-speed CMOS camera.

Figure 2 (a) shows schematic illustration of processes of impinging atomization and coordinate system of experiments. Origin of this coordinate system is impinging point of liquid jets. In order to clarify the effects of liquid jets velocities on spatial distribution of atomization characteristics, measurements on two different Weber number with liquid jets are conducted. The Webber numbers of those conditions are 1392 and 2474. PDA measurements are conducted in every 1 mm of *x*-*z* plane (from 0 mm to 15 mm in *x*-axis, from 2 mm to 22 mm in *z*-axis). Figure 2 (b) shows measurement area of PDA. The area above z = 2 mm cannot be measured because of the interference of laser beam by the injector holder. To compare the theoretical model and experimental results, the perpendicular spatial distributions of the atomization characteristics are measured at the height of z = 11, 18, 30 mm. Twenty thousand droplets are measured and analysed at each measuring point for statistical processing of PDA. Table 1 shows experimental conditions.

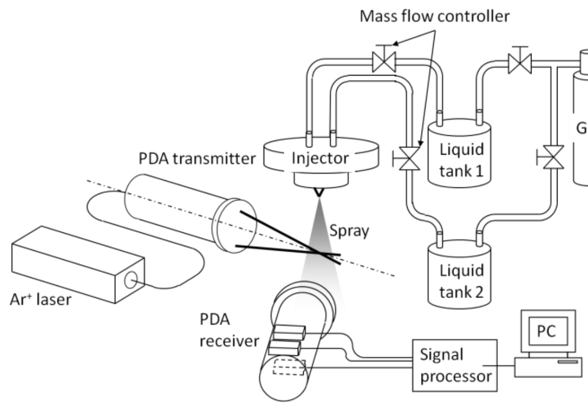

(a) Experimental apparatus with PDA system

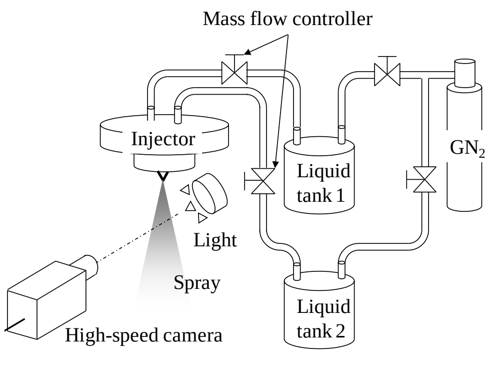

(b) Experimental apparatus with high-speed camera

Figure 1 Schematic illustration of experimental apparatus

Table 1 Experimental conditions

	Case1	Case2
Test Liquid	Water	
Ambient Pressure [MPa]	0.1	
Ambient Temperature [K]	Room temperature (293)	
Weber Number, We [-]	1392	2474
Number of sample droplets, [-]	20000	

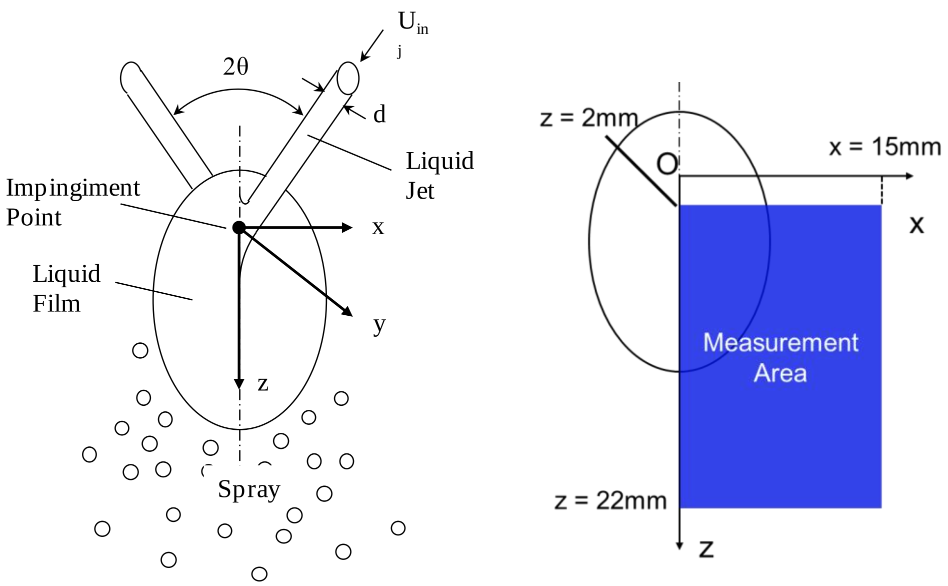

(a) Coordinate system (b) Measurement area

Figure 2 Schematic illustration of impinging jet atomization

Results and Discussion

・High speed direct imaging of impinging atomization processes

Since PDA cannot measure the droplet size at inside of liquid fan because of its measurement basics, it is needed to decide the edge of liquid fan in another way. In this experiment, the edge of liquid fan is decided through high speed imaging with using a back light. Figure 3 shows instantaneous direct photograph of impinging jet atomization of (a) Case1 (We = 1392) and (b) Case2 (We = 2474). Frame rate of these photographs are 3700 fps and the exposure time of these photographs are 10μs. Shadows appeared at upper part of photograph are huge droplets which are made by droplets' attaching at the nozzle. Those shadows should be neglect on this study. It can be found from Figs. 3 (a), (b) that there are typically breakup processes of impinging jet atomization. Those are "formation of liquid fan", "disintegration from liquid fan to the liquid fragments" and "breakup from liquid fragments into droplets". Moreover, a region of liquid fan and ligaments becomes smaller under high Weber number condition than that of low liquid velocity condition. These observations are same as previous reported theoretical results [1].

Figure 4 shows the measurement points in red grid. It is overlaying on Fig. 3. Each intersection points indicate the measurement points of PDA. In this study, we define the liquid fan as the edge of continuous fan. Blue dots as a liquid fan region and green dots as a ligament region are plotted in Fig. 4. Since the region of liquid fan and ligament region changes instantaneously, these regions are defined by using the largest area observed in high speed imaging. In addition, a disintegration line estimated by theoretical analysis [1] is also shown in Fig. 4 as a blue circle. This estimation is conducted with the same condition of experiments. It can be found from Fig. 4 that the liquid fans of experimental results are smaller than that of the theoretical analysis. This is because theoretical analysis deals with liquid sheet having smooth and homogeneous flow. In this experiment, liquid jet has inhomogeneous flow and it is impossible to keep shape of liquid jets because it is affected by the fluctuation of flow rate. Inoue et al. indicate that flow distribution of liquid jets affects flow distribution of liquid sheet, and formation of inflection point of flow distribution of liquid sheet advances atomization [27]. While it is difficult to measure flow field of liquid jets, it is considered that acceleration of instability of liquid sheet and liquid jet intensities disintegration of liquid sheet to droplets, and reduces liquid sheet.

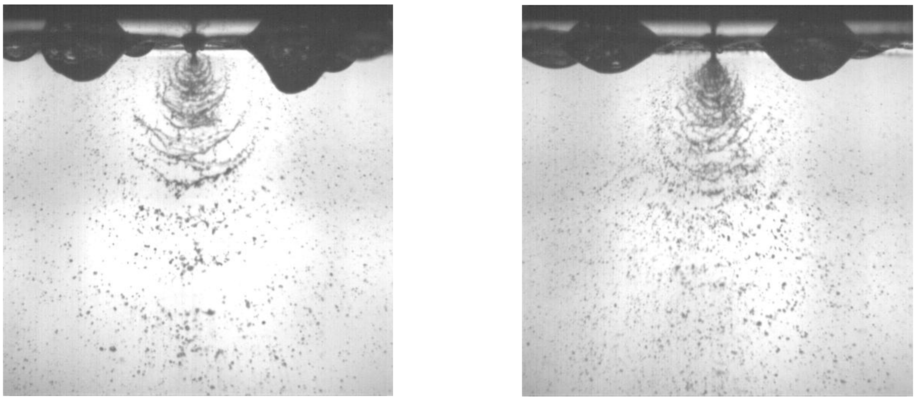

(a) Case 1 (b) Case2

Figure 3 instantaneous direct photographs of spray

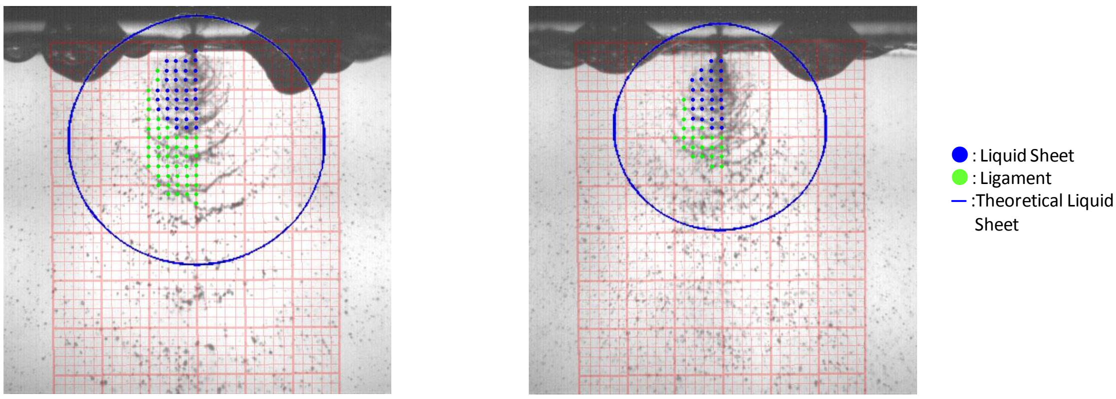

(a) Case 1 (b) Case2

Figure 4 Comparison of size of liquid sheet

・**Spatial distribution of spray characteristics of impinging atomization**

Figures 5 show contour maps of SMD in *x*-*z* plane with (a) Case1 and (b) Case2. Coordinates of Fig. 5 are same as given in Fig. 2 (a). The value of SMD has *z*-axis symmetric distribution. The white region appeared in Figs. 5 indicates the liquid fan region judged from the results as shown in Figs. 4 (a), (b). Since PDA cannot measure the droplet size at inside of liquid fan because of its measurement basics, the results in these areas are regarded as unreliable data. It is found from Figs. 5 (a), (b) that SMD decreases under high Weber number condition. Another feature recognized from Fig.5, the SMD increases with the increasing distance from the disintegration point. These tendencies stems from difference of flow velocity between liquid sheet and ambient air. It is found that SMD increases with increasing distance from impinging point. This is because droplet size distribution changes between each measuring points. Since small droplets have large evaporation rate and high traceability to the flow field, the probability density function of small droplets decrease with increasing distance between center point and liquid fan.

To clear up the variation of droplet size distribution, Figs. 6 (a) z = 11 mm and (b) 18 mm show the droplet size distribution at the different height of center axis in Case 2. Fig. 6 (a) shows droplet size distribution at edge of liquid fan, and Fig. 6 (b) shows droplet size distribution at the downstream of edge of liquid fan. The horizontal and vertical axes of Figs. 6 indicate the droplet size and the probability density function (PDF) of droplets, respectively. Fig. 6 (c) shows the subtraction of probability density function (PDF) of each measurement point (Fig. 6 (a) – Fig. 6 (b)). It is easily found from Fig. 6 (c) that the PDF under the size of 50 μm increases and the PDF of over 50 μm decreases with increasing the distance from impinging point, respectively. As a result, the SMD is increasing with increasing the distance from impinging point.

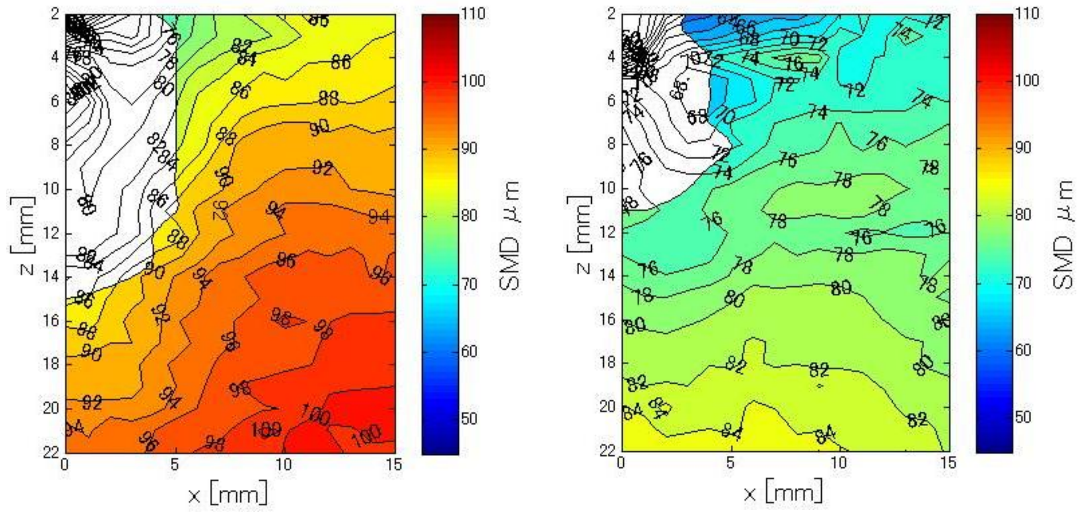

(a) Case 1 (b) Case2

Figure 5 Contour map of SMD

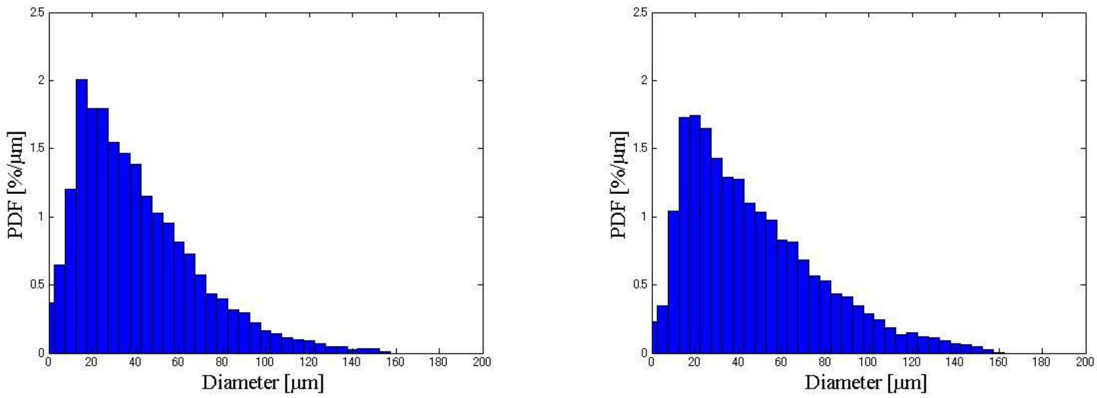

(a) z = 11 mm (a) z = 18 mm

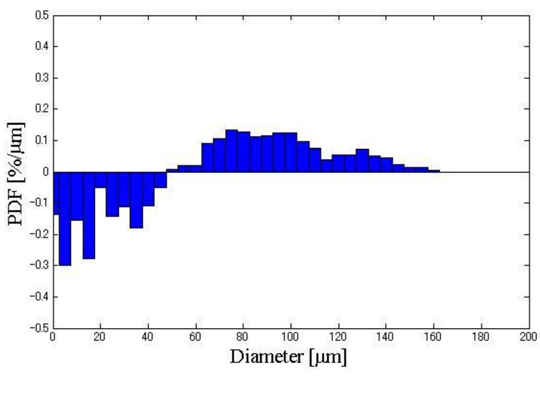

(c) Subtraction of droplet size distribution

Figure 6 Droplet size distributions

In addition, there are a lot of non-spherical droplets at the vicinity of liquid fan. Since large droplets need long time to get spherical, it is considered that the number of large droplets measured with PDA increases with increasing distance from liquid fan. Figure 9 shows the variation of SMD with changing the position on *z*-axis. It is found from Fig. 7 that SMD become constant at the enough distance.

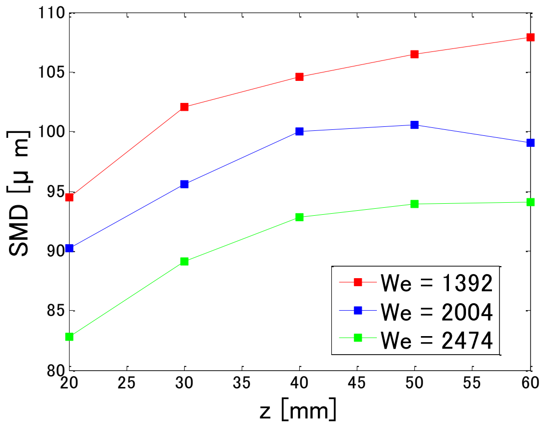

Figure 7 Variation of SMD with changing the position on *z*-axis.

Figure 8 shows contour map of SMD (Case 2) in *x*-*y* plane at (a) *z* = 11 mm, (b) 18 mm and (c) 30 mm. Figs. 8 indicates that there is little differences of SMD in *y*-direction at all height. Figures 8 (a) – (c) show mass flux contour map in *x*-*y* plane measured with PDA. Although it is known that value of the mass flux measured with PDA is inaccurate quantitatively, it should help us to understand distribution of the mass flux qualitatively. In Figs. 9 (a) and (b), there is high mass flux area around *z*-axis. In Fig. 9 (c), mass flux distribution is nearly flat. These tendencies indicate that mass flux distribution in perpendicular direction to the liquid fan is getting smooth with increasing distance from impinging point. From these results, it is possible to adapt impinging jet atomization model to actual phenomena by considering mass flux distributions.

These results indicate that the atomized spray is also distributed in *y*-direction and the droplet size distribution would be similar. Therefore, it can be thought that in order to improve the theoretical model, the distribution in *x*-*y* plane should be considered.

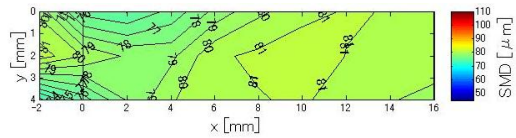

(a) *z* = 11mm

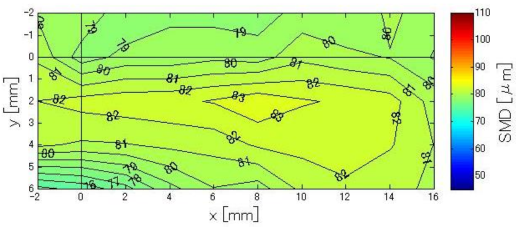

(b) *z* = 18mm

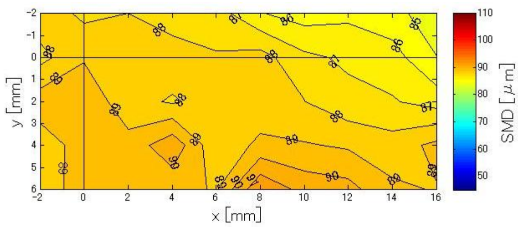

(c) *z* = 30mm

Figure 8 Contour map of SMD measured by PDA in *x*-*y* plane (Case 2)

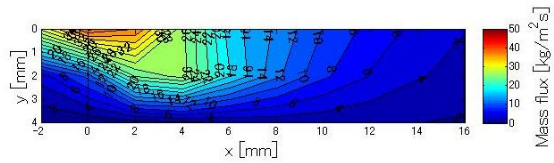

(a) *z* = 11mm

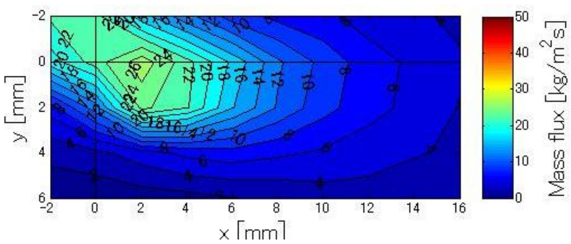

(b) *z* = 18mm

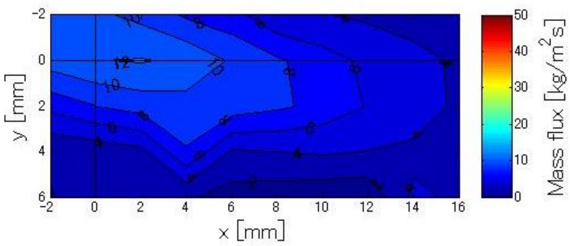

(c) *z* = 30mm

Figure 9 Contour map of mass flux measured by PDA in *x*-*y* plane (Case 2)

To confirm the variation of SMD at the vicinity of liquid fan, Figure 10 shows the variation of SMD measured in this experiment and numerical model with changing azimuthal angle. Azimuthal angle α means the angle between z-axis and measuring point. $\alpha = 0°$ means z-axis negative direction. Experimental values of Figure 10 are measured at the closest point to liquid fan which measured with high speed imaging. SMD cannot be measured the range where there are no experimental values resulted from the measurement area. As shown in Figure 10, it is found that SMD increases with increasing α and peaks at $\alpha = 180°$. This is because thickness of liquid sheet increases with increasing α. Numerical model denotes the same tendency of experimental value. However, there are differences between theoretical model and experimental results. The reason of this different is the same of reduction of liquid fan.

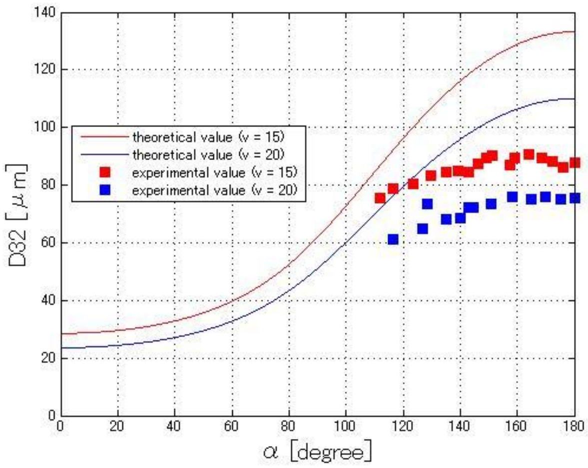

Figure 10 Variation of SMD with changing α

Summary and Conclusions

The final goal of this study is to make impinging jet atomization model with using atomization processes and spray characteristics at the vicinity of liquid fan. In order to make an impinging atomization model, we conducted experimental measurements by using high-speed imaging and phase Doppler anemometry at the vicinity of liquid fan. Results are summarized as follows.

And from the results of high-speed imaging, the liquid fans of experimental results are smaller than that of the theoretical analysis. This is because inhomogeneous flow and fluctuation of flow rate which is not considered in theoretical model. SMD did not change in y-direction at every height, but mass flux distribution is not flat at upper stream area.

Those results indicated that improving the atomization model in point of disintegration point and mass flux distribution, accurate atomization model could be proposed.

Acknowledgements

We gratefully acknowledge Dr. Kawahara from Okayama University for helping on high speed imaging.

References

[1] Inamura, T., Oguro, M., Kumakawa, A. and Tamura, H., Proceedings of the ILASS-Japan: 147-152 (2006).
[2] Greenberg, J. B., Albagli, D., Tambour, Y., *Combustion Science and Technology*: 50: 255-270 (1986).
[3] Chen, G., Gomez, A., *Proceedings of the Combustion Institute* 24: 1531-1539 (1992).
[4] Chen, N.-H., Rogg, B., Bray, K. N. C., *Proceedings of the Combustion Institute* 24: 1513-1521 (1992).
[5] Lacas, F., Darabiha, N., Versaevel, P., Rolon, J. C., Candel, S., *Proceedings of the Combustion Institute* 24: 1523-1529 (1992).
[6] Li, S. C., Libby, P. A., Williams, F. A., *Proceedings of the Combustion Institute* 24: 1503-1512. (1992)
[7] Darabiha, N., Lacas, F., Rolon, J. C., Candel, S., *Combustion and Flame* 95: 261-275. (1993)
[8] Greenberg, J. B., Sarig, N., *Combustion Science and Technology* 92: 1-33 (1993).
[9] Gutheil, E., *Combustion and Flame* 93: 239-254 (1993).
[10] Li, S. C., Libby, P. A., Williams, F. A., *Combustion and Flame* 94: 161-177 (1993).
[11] Greenberg, J. B., Sarig, N., *Combustion and Flame* 104: 431-459 (1996).
[12] Greenberg, J. B., Sarig, N., *Proceedings on the Combustion Institute* 26: 1705-1711 (1996).
[13] Li, S. C., *Progress in Energy and Combustion Science* 23: 303-347 (1997).

[14] Gutheil, E., Sirignano, W. A., *Combustion and Flame* 113: 92-105 (1998).
[15] Massot, M., Kumar, M., Smooke, M. D., Gomez, A., *Proceedings of the Combustion Institute* 27: 1975-1983, (1998).
[16] Li, S. C., Williams, F. A., *Proceedings of the Combustion Institute* 28: 1031-1038 (2000).
[17] Santoro, V. S., Kyritsis, D. C., Gomez, A., *Proceedings of the Combustion Institute* 28: 1023-1030 (2000).
[18] Bossard, J. A., Peck, R. E., Proceedings of the Combustion Institute 26: 1671-1677 (1996).
[19] Dombrowski, N. and Johns, W. R., *Chemical Engineering Science*: 203-214 (1963).
[20] Chiu, H. H., Jiang, T. L., Berry, G. F. and Croke, E. J., *U. S. Doe Reports*, CONF8610210, (1986).
[21] Jiang, T. L., Chiang, W. T. and Jang S. D., *AIAA/SAE/ASME/ASEE 28th Joint Propulsion Conference and Exhibit*, AIAA 92-3769, (1992).
[22] Gray, H. L., *AIAA/SAE/ASME/ASEE 28th Joint Propulsion Conference and Exhibit*, AIAA 92-3765, (1992).
[23] Krishnan, A., Przekwas, A. J. and Gross, K. W., *AIAA Space Programs and Technologies Conference*, AIAA 92-1552, (1992).
[24] Larosiliere, L. M., Litchford, R. J. and Jeng, S., *AIAA/SAE/ASME/ASEE 26th Joint Propulsion Conference and Exhibit*, AIAA 90-2238, (1990).
[25] Ryan H. M., Anderson, W. E., Pal, S. and Santoro, R. J., *Journal of Propulsion and Power*, Vol. 11, No. 1: 135-145 (1995).
[26] Strakey, P. A, Talley, D. G., *Eighth International Conference on Liquid Atomization and Spray Systems*: (2000)
[27] Inoue, C., Watanabe, T. and Himeno, T., *45th AIAA/ASME/SAE/ASEE Joint Propulsion Conference and Exhibit*, AIAA-2009-5041, (2009).